Solar wind density controlling penetration electric field at the equatorial ionosphere during a saturation of cross polar cap potential

Y. Wei,[1,2] W. Wan,[2] B. Zhao,[2] M. Hong,[2] A. Ridley,[3] Z. Ren,[2] M. Fraenz,[1] E. Dubinin,[1] and M. He[4]

Received 5 February 2012; revised 26 July 2012; accepted 2 August 2012; published 14 September 2012.

[1] The most important source of electrodynamic disturbances in the equatorial ionosphere during the main phase of a storm is the prompt penetration electric field (PPEF) originating from the high-latitude region. It has been known that such an electric field is correlated with the magnetospheric convection or interplanetary electric field. Here we show a unique case, in which the electric field disturbance in the equatorial ionosphere cannot be interpreted by this concept. During the superstorm on Nov. 20–21, 2003, the cross polar cap potential (CPCP) saturated at least for 8.2 h. The CPCP reconstructed by Assimilative Mapping of Ionospheric Electrodynamics (AMIE) procedure suggested that the PPEF at the equatorial ionosphere still correlated with the saturated CPCP, but the CPCP was controlled by the solar wind density instead of the interplanetary electric field. However, the predicted CPCPs by Hill-Siscoe-Ober (HSO) model and Boyle-Ridley (BR) model were not fully consistent with the AMIE result and PPEF. The PPEF also decoupled from the convection electric field in the magnetotail. Due to the decoupling, the electric field in the ring current was not able to comply with the variations of PPEF, and this resulted in a long-duration electric field penetration without shielding.

Citation: Wei, Y., W. Wan, B. Zhao, M. Hong, A. Ridley, Z. Ren, M. Fraenz, E. Dubinin, and M. He (2012), Solar wind density controlling penetration electric field at the equatorial ionosphere during a saturation of cross polar cap potential, *J. Geophys. Res.*, *117*, A09308, doi:10.1029/2012JA017597.

1. Introduction

[2] The prompt penetration electric field (PPEF) has been shown in previous studies to be driven by the interplanetary electric field (IEF) or convection electric field [*Wolf et al.*, 2007; *Fejer*, 2011]. This concept has been confirmed with comprehensive data set during moderate storms [e.g., *Kelley et al.*, 2003; *Wei et al.*, 2008a, 2011a], intense storms [e.g., *Huang et al.*, 2005; *Guo et al.*, 2011] and superstorms [e.g., *Fejer et al.*, 2007; *Kikuchi et al.*, 2008; *Tsurutani et al.*, 2008; *Zhao et al.*, 2005, 2008]. However, because superstorms "create extremely enhanced electromagnetic fields and particle environments that behave differently than that predicted by conventional theory" [*Bell et al.*, 1997], the PPEF during some superstorms may exhibit some unexpected features. For example, *Huang et al.* [2005] concluded that during the main phases of some intense storms IEF can penetrate without attenuation into the equatorial ionosphere for several hours, but *Fejer et al.* [2007] found that the PPEF during the main phase of the superstorm on November 9, 2004 was not proportional to the IEF and cross polar cap potential (CPCP).

[3] The most severe superstorm of solar cycle 23 took place during November 20–21, 2003, featuring the lowest Dst (−472 nT) and SYMH (−490 nT) in this solar cycle (Figure 1a). Indeed, there were some unusual observations during this superstorm. *Hori et al.* [2006] reported a highly turbulent convection electric field in the magnetotail, which was inconsistent with the IEF pattern. They further suggested that the convection electric field in the near-Earth tail and the electric field in the inner magnetosphere decoupled from each other. Some unique attributions of the ionospheric response to this superstorm have also been revealed through the ground- and space-based instruments [*Zhao et al.*, 2012, and reference therein]. For example, the DMSP-F13 spacecraft shows definite evidence of saturation of the cross polar cap potential drop in the Earth's ionosphere [*Hairston et al.*, 2005]. The dayside source of the polar tongue of ionization (TOI) has been proved to be the plume of storm enhanced density transported from low latitudes in the post-noon sector by the subauroral disturbance electric field using the

[1]Max Planck Institute for Solar System Research, Katlenburg-Lindau, Germany.
[2]Beijing National Observatory of Space Environment, Institute of Geology and Geophysics, Chinese Academy of Sciences, Beijing, China.
[3]Department of Atmospheric, Oceanic, and Space Sciences, University of Michigan, Ann Arbor, Michigan, USA.
[4]School of Engineering and Science, Jacobs University Bremen, Bremen, Germany.

Corresponding author: Y. Wei, Max Planck Institute for Solar System Research, Max-Planck-Str. 2, 37191 Katlenburg-Lindau, Germany. (wei@mps.mpg.de)

0148-0227/12/2012JA017597

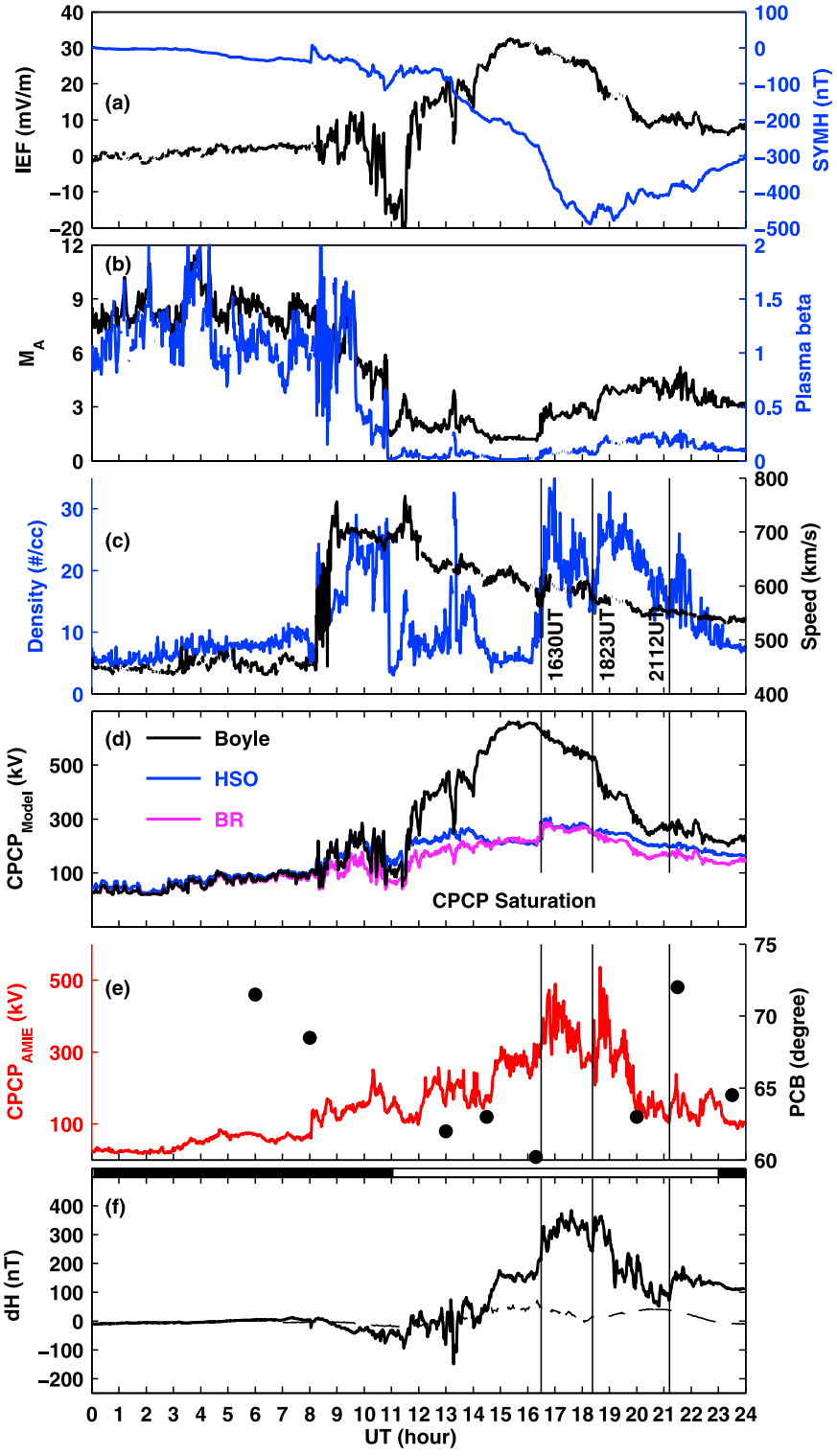

Figure 1. (a) IEF (black) and symmetric ring current index (SYMH); (b) solar wind Mach number (M_A) and plasma beta (red); (c) solar wind density (blue) and speed; (d) the cross polar cap potentials (CPCPs) predicted by Boyle model, HSO model and BR model, respectively (see the text for references); (e) the CPCP calculated by AMIE procedure and the polar cap boundary measured by DMSP F13; (f) the ΔH inferred from two geomagnetometers' observation in Peru. The dashed line is quiet level measured on November 19 for a reference. The black/white bar illustrates local nightside/dayside interval. The three vertical lines demonstrate the evidence for the control by solar wind of the CPCP and penetration electric field in the equatorial ionosphere.

global GPS network and SuperDARN and DMSP observations [*Foster et al.*, 2005].

[4] Here we examine the relation of PPEF with IEF and CPCP during the November 20–21, 2003 superstorm. The CPCP is estimated by four methods: Boyle model [*Boyle et al.*, 1997], Hill-Siscoe-Ober (HSO) model [*Ober et al.*, 2003], Boyle-Ridley (BR) model [*Ridley*, 2005] and Assimilative Mapping of Ionospheric Electrodynamics (AMIE) procedure [*Richmond and Kamide*, 1988; *Ridley and Kihn*, 2004]. The Boyle, HSO and BR model are constructed based on different physical pictures, but all of them take solar wind parameters as input to predict CPCP; The AMIE procedure uses observed ionospheric parameters to reconstruct CPCP. Therefore, comparison of their performances with the observed PPEF is expected to provide some clues to understand the solar wind-magnetosphere-ionosphere coupling during superstorms.

2. Observations

[5] Figures 1a–1c show the 1-min resolution solar wind parameters: Y component of the IEF in GSM coordinates, Alfven Mach Number, plasma beta, solar wind density and speed. The data from the "OMNI" database are derived from ACE observations at L1 point and are shifted to the subsolar magnetosphere. The consequences of the large IEF can be seen in SYMH (Figure 1a) and the lowest latitude of the polar cap boundary (PCB) (Figure 1e) determined on the dawnside and duskside based on the DMSP F13 observations in the Northern Hemisphere [*Ebihara et al.*, 2005]. It shows that the polar cap expanded when the strength of IEF increased before 1600 UT and then shrank when the strength gradually decreased.

[6] Figure 1d illustrates the predicted CPCPs by Boyle, HSO and BR model with 1-min resolution. The Boyle model assumes a linear relationship between the interplanetary magnetic field (IMF) and the CPCP, and thus predicts an unrealistically high CPCP due to the strong IEF. Comparing to the $CPCP_{Boyle}$, the HSO and BR models show smaller CPCPs at the same time. This is because the HSO and BR model considers the so-called saturation effect [e.g., *Shepherd*, 2007]. Both HSO model and BR model predict a strong CPCP saturation effect during the main phase (1131–1944 UT) of the storm, as seen from the significant discrepancy from $CPCP_{Boyle}$. Note that the $CPCP_{HSO}$ has been found to be consistent with the DMSP satellite observations [*Ebihara et al.*, 2005]. The fourth method for evaluating the CPCP, the AMIE procedure, is a technique used to reconstruct the high-latitude ionospheric electrodynamic parameters by combining the various data sets [*Richmond and Kamide*, 1988; *Ridley and Kihn*, 2004]. Figure 1e shows that the pattern of $CPCP_{AMIE}$ is fairly consistent with $CPCP_{HSO}$ and $CPCP_{BR}$, especially the jump at 1630 UT. Nevertheless, $CPCP_{AMIE}$ showed two other notable jumps at 1823 and 2112 UT, but none of the former models predicts these jumps. In other words, the physical processes responsible for the two jumps have not been correctly emphasized or even not included in the theoretical models.

[7] The daytime equatorial ionospheric electric field can be inferred from the difference between geomagnetic H components (ΔH) of a pair of stations, of which one is located near the geomagnetic equator and the other one is located off the equator [*Anderson et al.*, 2002]. Here we choose two stations in Peru (LT = UT − 5 h): Jicamarca (JIC, 11.9°S, 76.9°W, dip 0.8°N) and Piura (PIU, 5.2°S, 79.6°W, dip 6.8°N). Figure 1f illustrates the 1-min ΔH data. The positive (negative) value of ΔH denotes eastward (westward) equatorial electric field. The large eastward electric field on November 20 was mainly contributed by the PPEF, because the eastward solar quiet (Sq) field component, produced by the neutral wind dynamo, was negligible if we assume that it was roughly the same as that on the quiet day November 19 (dashed line). The ΔH started to increase at 1400 UT (0900 LT) and persisted for about 7 h indicating a long lasting PPEF event. Before 1400 UT, ΔH is small due to the low Cowling conductivity during sunrise period. Actually, the PPEF takes pronounced effect in the ionosphere 2 h earlier than ΔH associated with the increment of IEF at 1200–1400 UT at the East Asian longitude (LT = UT + 8). This is proved by a drastic elevation of the equatorial ionosphere as observed by *Zhao et al.* [2008] which found that the eastward PPEF during this storm occurred during the nighttime hours of 2000–2200 LT. Thus it appears that there is no evident delay between the IEF and PPEF in the ionosphere as described by *Mannucci et al.* [2008].

[8] Of interest here is that the eastward electric field started to increase at the beginning of recovery phase associated with gradual decrease of IEF. Note that the eastward equatorial electric field often starts to decrease or even change to westward during recovery phase of many intense storms [e.g., *Huang et al.*, 2005] and some superstorms [e.g., *Kikuchi et al.*, 2008]. There are two possible mechanisms for the reduction of equatorial electric field: (1) westward electric field produced by the disturbance dynamo, which usually takes several hours to become effective and is more significant on the nightside [*Fejer*, 2011]; (2) effective westward shielding electric field. But none of them likely took effect in our event because the observations showed an enhancement of eastward electric field rather than reduction.

[9] The vertical lines mark three jumps in ΔH, which match the increases in $CPCP_{AMIE}$. This feature still supports the well-known concept that the convection electric field in the polar ionosphere penetrates to the equatorial ionosphere. However, we found the corresponding variations in the solar wind exclusively existed in the density rather than the IEF and speed. Therefore, the solar wind density instead of the IEF controlled the polar convection electric field and then the PPEF. Figure 2 (bottom) gives a closer view of the solar wind dynamic pressure (SWDP), $CPCP_{AMIE}$ and the equatorial electric field. In order to show their consistence, the $CPCP_{AMIE}$ was scaled to match the E_{J_P} shape. Since the solar wind speed was quite stable, the SWDP can also represent the variations in the density. The equatorial ionospheric electric field E_{J_P} was derived from the ΔH, according to the linear relationship $E_{J-P} = (\Delta H - 14)/2.3/40$ suggested by *Anderson et al.* [2002]. The derived value varied between 3–4 mV/m during 1630–1900 UT, which is significantly larger than the averaged quiet-day value 0.63 mV/m in this region during the daytime [*Fejer*, 2011]. The large eastward electric field can be confirmed by the response of the ionospheric electrodynamic processes as seen from the 15-min resolution ionospheric profilograms at Jicamarca (Figure 2, middle). The Digisonde ionospheric profilograms show the

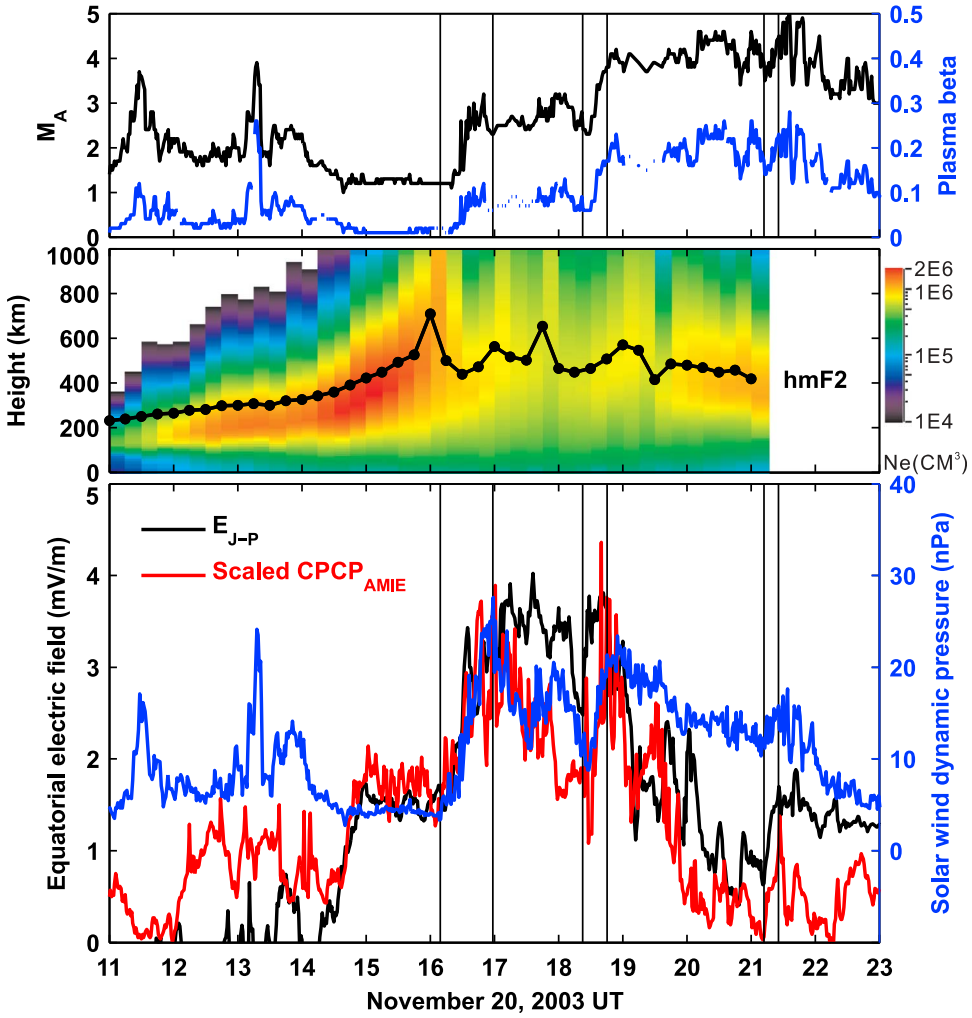

Figure 2. (top) Zoom-in view of the M_A and plasma beta; (middle) profilograms from the Digisonde at Jicamarca, and the F2 peak altitude hmF2; and (bottom) the observed equatorial electric field, scaled $CPCP_{AMIE}$ and solar wind dynamic pressure.

ionogram-derived electron density profiles, Ne(h), as functions of time, where color coding is used to represent the plasma density. The large eastward PPEF lifted up the original F2 layer even beyond 1000 km and a new F2 layer forms at the bottomside, creating false collapse of hmF2, which is a common feature during the superstorm [e.g., *Zhao et al.*, 2005; *Paznukhov et al.*, 2007].

3. Discussion

3.1. Why There Was No Shielding

[10] The observations suggest that the PPEF originated from the polar convection electric field even when the CPCP saturated. This is still consistent with the classical scenario of electric field penetration. However, the CPCP decoupled from the IEF, but coupled to the solar wind density. This phenomenon cannot be explained by the classical scenario. Viewing from the magnetosphere, in the classical scenario [*Vasyliunas*, 1972; *Wolf et al.*, 2007], the PPEF in the inner magnetosphere is caused by the magnetospheric convection electric field, while the ring current tends to shield the inner magnetosphere from the convection electric field. An enhancement of plasma convection will cause an azimuthal gradient of plasma pressure in the ring current, which gives rise to a westward electric field. The westward electric field tends to reduce the eastward convection electric field, thus it seems to "shield" the inner magnetosphere from the enhanced convection electric field. The terms "undershielding," "goodshielding" and "overshielding" refer to the situations that westward shielding electric field is smaller than, equal to and larger than eastward PPEF, respectively [*Wei et al.*, 2010, 2011b]. Therefore, both the penetration electric field and the shielding electric field are products of the magnetospheric convection electric field, with the latter always adjusting to comply with the PPEF until the PPEF is mostly canceled. Viewing from the ionosphere, the classical scenario works well in explaining the observations by simply mapping these electric fields from magnetosphere to ionosphere along the field lines.

[11] However, for our event, *Hori et al.* [2006] found that the fluctuating convection electric field in the near-Earth tail decoupled from the electric field in the inner magnetosphere,

while we observed that the PPEF still originated from the polar convection electric field. If we assume that the electric field in the inner magnetosphere still coupled with the PPEF in the mid- and low-latitude ionosphere by mapping along the closed field line, what has become clear is that the convection electric field in the polar ionosphere was not fully produced by the convection electric field in the magnetotail. This point is consistent with present understanding of CPCP saturation: Though the full physical picture of CPCP saturation is still hotly debated so far, a consensus is that the strength of the region 1 field aligned current (R1 FAC) system associated with the CPCP must be limited [*Siscoe et al.*, 2004]. Therefore, the dominant source of the PPEF and polar convection electric field must be directly related to the solar wind density without communication to the magnetotail. In other words, the source is expected to directly come from the interaction between solar wind and the dayside magnetopause instead of global plasma convection. Since the PPEF is no longer a product of the magnetospheric convection electric field, the shielding mechanism taking place in the ring current cannot comply with the variation of PPEF, i.e., there is no normal shielding. As a result, the PPEF persisted for at least 8 h (1400–2200UT) as identified from the similar variations in E_{J_P} and $CPCP_{AMIE}$.

3.2. Solar Wind Density and Saturated CPCP

[12] The PPEF and the solar wind density exhibited similar variations when the CPCP was in saturation regime. We turn to the question how the solar wind density causes an increase in the saturated CPCP. The previous works on this issue usually discuss the role of solar wind density as SWDP and Alfven Mach number. The HSO model expresses the effect of solar wind density as SWDP, while the BR model considers the combined effect of Mach number and SWDP. *Boudouridis et al.* [2004] analyzed a case that an enhancement of SWDP caused an increase of CPCP in the saturation regime. When the Ober contribution to the HSO model was taken into account, they found that the CPCP for the lower pressure level was similar to observations, but not for the high pressure level. On the other hand, both the general (not limited to CPCP saturation case) statistical work by *Yu and Ridley* [2011] and a case study by *Boudouridis et al.* [2008] revealed that the CPCP changes dramatically in the first few minutes after the SWDP increases, and can then remain elevated for a long time afterwards (sometimes for 1–2 h). This feature also appeared in our event. As shown in Figure 2 (bottom), the SWDP was decreasing during 1700–1740 UT, and the $CPCP_{AMIE}$ was also following this tendency, but the PPEF remained elevated. This suggested that the physical processes inside the magnetosphere still play an important role after a SWDP enhancement, no matter whether the CPCP is in the saturation regime or not.

[13] From the view of Mach number, *Lopez et al.* [2004] proposed that during low Mach number period the solar wind density and the magnetic field strength control the compression ratio of the bow shock. During nominal solar wind and IMF conditions, the magnetic field is always increased by approximately a factor of four (independent of the solar wind density, as long as the Mach number is above four) as it goes through the shock. As the magnetic field increases, and the Mach number goes down, there is less and less compression across the bow shock, thereby reducing the effective magnetic energy in the sheath. On the other hand, if the Mach number is low already, an increase in the density corresponds to an increase in the Mach number, and it will increase the compression ratio across the shock toward nominal values. This effect has been included in the BR model [*Ridley*, 2005], and the model indeed successfully predicted the largest increase in CPCP at 1630 UT (Figure 1d). However, both HSO (considers SWDP) and BR model (considers SWDP and Mach number) miss the other two increases in $CPCP_{AMIE}$ at 1823 UT and 2112 UT, implying that more parameters need to be considered together with SWDP and Mach number.

[14] Recently, several studies have tried to investigate the relation between the plasma beta and the CPCP saturation for both southward IMF (R.E. Lopez, personal communication, 2009) and northward IMF (for the reversed plasma convection) [*Wilder et al.*, 2009], and they suggested that as the beta increases, the CPCP over the saturated regime also seems to increase. This is consistent with our observations (Figure 2). Furthermore, according to the observations shown by *Wilder et al.* [2009, Figure 14], the plasma beta of <0.3 (in our case) is in a range which has a high probability for CPCP saturation. However, a similar study of beta-dependence for southward IMF has not been performed.

3.3. General Comments on Relation Between Solar Wind Dynamic Pressure and PPEF

[15] We have shown that the solar wind density was related to the PPEF when the IEF was extremely strong and the CPCP was in saturation regime. Since the solar wind speed in our event was quite stable, we are allowed to discuss the effect of SWDP with these observations. Actually, the effects of SWDP on the mid-ionosphere had been found during moderate and intense storm time, even northward IMF period [e.g., *Huang et al.*, 2002, 2008; *Yuan and Deng*, 2007; *Wei et al.*, 2008b, 2011a; *Zong et al.*, 2010]. All these observations tell us, PPEF is usually enhanced as response to an enhancement of solar wind dynamic pressure, no matter whether the storm is a superstorm or not.

[16] However, the physical processes underlying the response could be very different for non-superstorms and superstorm periods. For the former, *Huang et al.* [2008] discussed two possible mechanisms: (1) the solar wind shock causes an over-compression of the magnetosphere, and (2) the field-aligned and ionospheric currents driven by the solar wind shock cause the enhancements of the ionospheric electric and magnetic fields. Yet they concluded that neither of the mechanisms appears to be able to provide a complete explanation of all observed features. On the other hand, *Wei et al.* [2008b] suggested that the "magnetospheric configuration" (see the review by *Fejer* [2011]) could be the most important processes to affect PPEF at equator. These ideas imply that the dominant processes take place inside the magnetosphere. But for our superstorm event, as discussed above, our explanation denotes that the dominant processes are outside and on the magnetopause.

[17] Finally, we should remind that the sources of the disturbed equatorial ionospheric electric field are far more complicated as revealed by comprehensive observations. Also in a superstorm, *Fejer et al.* [2007] found that the PPEF during the main phase of the superstorm was neither proportional to the solar wind electric fields nor to the CPCP.

Some substorms are found to be able to produce disturbances at equator [e.g., *Wei et al.*, 2009]. Especially, the polar cap area may be also important for the strength of PPEF at the equator. Given polar cap electric field, the strength of PPEF can be determined with penetration efficiency (ratio of equatorial PPEF to polar electric field), which varies with local time and global distribution of ionospheric conductivity [*Wei et al.*, 2008c]. However, assuming a constant CPCP, the polar electric field will increase when polar cap shrinks, thus the PPEF increases. Consequently, the strength of PPEF is affected by the polar cap area, even assuming that the other factors are constant. For the November, 2004 superstorm, the penetration efficiency has been observed to be highly variable even during the daytime [*Fejer et al.*, 2007]. For our event, the shrinkage of polar cap may contribute to the enhancement of PPEF during recovery phase.

4. Conclusion

[18] The observations during the November 20, 2003 superstorm show the CPCP was being strongly saturated for a long time (8.2 h). During the saturation period, (1) the PPEF in the equatorial ionosphere was consistent with the CPCP derived by AMIE procedure; (2) the PPEF decoupled from the IEF and also the fluctuating convection electric field in the near-Earth magnetotail, which was published by *Hori et al.* [2006]; (3) the PPEF was enhanced when the solar wind density increased; (4) the shielding mechanism did not work for at least 8 h.

[19] With the observations shown in this paper and presented by the other references, we have proposed an explanation for PPEF enhancement driven by solar wind density enhancement. When the CPCP was in the saturation regime, the source of the increment of PPEF is expected to directly come from the interaction between solar wind and the dayside magnetopause instead of magnetospheric plasma convection. Since the PPEF is no longer a product of the magnetospheric convection electric field, the classical shielding mechanism taking place in the ring current cannot comply with the variation of PPEF, and thus there is no normal shielding. Consequently, the PPEF persisted for at least 8 h.

[20] The full physical picture underneath the relation between the solar wind density and the PPEF cannot be clearly identified, but they should be described by a combination of several plasma parameters often used, such as solar wind dynamic pressure, Alfven Mach number and plasma beta.

[21] **Acknowledgments.** This work is supported by grant WO910/3–1 within the priority program "Planetary Magnetism" of the Deutsche Forschungsgemeinschaft (DFG) and grant 50QM0801 of the German Aerospace Agency (DLR). The work in China was supported by National Science Foundation of China (41004072, 41174138) and National Important Basic Research Project (2011CB811405). We gratefully acknowledge the Center for Space Sciences at the University of Texas at Dallas and the U.S. Air Force for providing the DMSP thermal plasma data. We acknowledge the CDAWeb for access to the OMNI data. The SYMH, ASYD and AE data are provided by the World Data Center for Geomagnetism at Kyoto University. The Jicamarca Radio Observatory is a facility of the Instituto Geofisico del Perú operated with support from the NSF Cooperative Agreement ATM-0432565 through Cornell University.

[22] Philippa Browning thanks the reviewers for their assistance in evaluating this paper.

References

Anderson, D., A. Anghel, K. Yumoto, M. Ishitsuka, and E. Kudeki (2002), Estimating daytime vertical E × B drift velocities in the equatorial F-region using ground-based magnetometer observations, *Geophys. Res. Lett.*, *29*(12), 1596, doi:10.1029/2001GL014562.

Bell, J., M. Gussenhoven, and E. Mullen (1997), Super storms, *J. Geophys. Res.*, *102*(A7), 14,189–14,198, doi:10.1029/96JA03759.

Boudouridis, A., E. Zesta, L. R. Lyons, and P. C. Anderson (2004), Evaluation of the Hill-Siscoe transpolar potential saturation model during a solar wind dynamic pressure pulse, *Geophys. Res. Lett.*, *31*, L23802, doi:10.1029/2004GL021252.

Boudouridis, A., E. Zesta, L. R. Lyons, P. C. Anderson, and A. J. Ridley (2008), Temporal evolution of the transpolar potential after a sharp enhancement in solar wind dynamic pressure, *Geophys. Res. Lett.*, *35*, L02101, doi:10.1029/2007GL031766.

Boyle, C., P. Reiff, and M. Hairston (1997), Empirical polar cap potentials, *J. Geophys. Res.*, *102*, 111–125, doi:10.1029/96JA01742.

Ebihara, Y., M.-C. Fok, S. Sazykin, M. F. Thomsen, M. R. Hairston, D. S. Evans, F. J. Rich, and M. Ejiri (2005), Ring current and the magnetosphere-ionosphere coupling during the superstorm of 20 November 2003, *J. Geophys. Res.*, *110*, A09S22, doi:10.1029/2004JA010924.

Fejer, B. G. (2011), Low latitude ionospheric electrodynamics, *Space Sci. Rev.*, *158*, 145–166, doi:10.1007/s11214-010-9690-7.

Fejer, B. G., J. W. Jensen, T. Kikuchi, M. A. Abdu, and J. L. Chau (2007), Equatorial ionospheric electric fields during the November 2004 magnetic storm, *J. Geophys. Res.*, *112*, A10304, doi:10.1029/2007JA012376.

Foster, J. C., et al. (2005), Multiradar observations of the polar tongue of ionization, *J. Geophys. Res.*, *110*, A09S31, doi:10.1029/2004JA010928.

Guo, J., X. Feng, P. Zuo, J. Zhang, Y. Wei, and Q. Zong (2011), Interplanetary drivers of ionospheric prompt penetration electric fields, *J. Atmos. Sol. Terr. Phys.*, *73*, 130–136, doi:10.1016/j.jastp.2010.01.010.

Hairston, M. R., K. A. Drake, and R. Skoug (2005), Saturation of the ionospheric polar cap potential during the October–November 2003 superstorms, *J. Geophys. Res.*, *110*, A09S26, doi:10.1029/2004JA010864.

Hori, T., A. T. Y. Lui, S. Ohtani, P. C. Brandt, B. H. Mauk, R. W. McEntire, K. Maezawa, T. Mukai, Y. Kasaba, and H. Hayakawa (2006), Convection electric field in the near-Earth tail during the super magnetic storm of November 20–21, 2003, *Geophys. Res. Lett.*, *33*, L21107, doi:10.1029/2006GL027024.

Huang, C.-S., J. C. Foster, and P. J. Erickson (2002), Effects of solar wind variations on the midlatitude ionosphere, *J. Geophys. Res.*, *107*(A8), 1192, doi:10.1029/2001JA009025.

Huang, C. S., J. C. Foster, and M. C. Kelley (2005), Long-duration penetration of interplanetary electric field to the low latitude ionosphere during the main phase of magnetic storms, *J. Geophys. Res.*, *110*, A11309, doi:10.1029/2005JA011202.

Huang, C.-S., K. Yumoto, S. Abe, and G. Sofko (2008), Low-latitude ionospheric electric and magnetic field disturbances in response to solar wind pressure enhancements, *J. Geophys. Res.*, *113*, A08314, doi:10.1029/2007JA012940.

Kelley, M. C., J. J. Makela, J. L. Chau, and M. J. Nicolls (2003), Penetration of the solar wind electric field into the magnetosphere/ionosphere system, *Geophys. Res. Lett.*, *30*(4), 1158, doi:10.1029/2002GL016321.

Kikuchi, T., K. K. Hashimoto, and K. Nozaki (2008), Penetration of magnetospheric electric fields to the equator during a geomagnetic storm, *J. Geophys. Res.*, *113*, A06214, doi:10.1029/2007JA012628.

Lopez, R. E., M. Wiltberger, S. Hernandez, and J. G. Lyon (2004), Solar wind density control of energy transfer to the magnetosphere, *Geophys. Res. Lett.*, *31*, L08804, doi:10.1029/2003GL018780.

Mannucci, A. J., B. T. Tsurutani, M. A. Abdu, W. D. Gonzalez, A. Komjathy, E. Echer, B. A. Iijima, G. Crowley, and D. Anderson (2008), Superposed epoch analysis of the dayside ionospheric response to four intense geomagnetic storms, *J. Geophys. Res.*, *113*, A00A02, doi:10.1029/2007JA012732.

Ober, D. M., N. C. Maynard, and W. J. Burke (2003), Testing the Hill model of transpolar potential saturation with observations, *J. Geophys. Res.*, *108*(A12), 1467, doi:10.1029/2003JA010154.

Paznukhov, V. V., B. W. Reinisch, P. Song, X. Huang, T. W. Bullett, and O. Veliz (2007), Formation of an F3 layer in the equatorial ionosphere: A result from strong IMF changes, *J. Atmos. Sol. Terr. Phys.*, *69*, 1292–1304, doi:10.1016/j.jastp.2006.08.019.

Richmond, A. D., and Y. Kamide (1988), Mapping electrodynamic features of the high-latitude ionosphere from localized observations: Technique, *J. Geophys. Res.*, *93*, 5741–5759, doi:10.1029/JA093iA06p05741.

Ridley, A. J. (2005), A new formulation for the ionospheric cross polar cap potential including saturation effects, *Ann. Geophys.*, *23*, 3533–3547, doi:10.5194/angeo-23-3533-2005.

Ridley, A. J., and E. A. Kihn (2004), Polar cap index comparisons with AMIE cross polar cap potential, electric field, and polar cap area, *Geophys. Res. Lett.*, *31*, L07801, doi:10.1029/2003GL019113.

Shepherd, S. G. (2007), Polar cap potential saturation: Observations, theory, and modeling, *J. Atmos. Sol. Terr. Phys.*, *69*, 234–248, doi:10.1016/j.jastp.2006.07.022.

Siscoe, G., J. Raeder, and A. J. Ridley (2004), Transpolar potential saturation models compared, *J. Geophys. Res.*, *109*, A09203, doi:10.1029/2003JA010318.

Tsurutani, B., et al. (2008), Prompt penetration electric fields (PPEFs) and their ionospheric effects during the great magnetic storm of 30–31 October 2003, *J. Geophys. Res.*, *113*, A05311, doi:10.1029/2007JA012879.

Vasyliunas, V. (1972), The relationship of magnetospheric processes, in *Earth's Magnetospheric Processes*, edited by B. M. McCormac, pp. 29–38, Springer, New York, doi:10.1007/978-94-010-2896-7_3.

Wei, Y., et al. (2008a), Unusually long lasting multiple penetration of interplanetary electric field to equatorial ionosphere under oscillating IMF B_z, *Geophys. Res. Lett.*, *35*, L02102, doi:10.1029/2007GL032305.

Wei, Y., M. Hong, W. Wan, A. Du, Z. Pu, M. F. Thomsen, Z. Ren, and G. D. Reeves (2008b), Coordinated observations of magnetospheric reconfiguration during an overshielding event, *Geophys. Res. Lett.*, *35*, L15109, doi:10.1029/2008GL033972.

Wei, Y., M. H. Hong, W. X. Wan, and A. M. Du (2008c), A modeling study of interplanetary-equatorial electric field penetration efficiency, *Chin. J. Geophys.*, *51*, 1279–1284.

Wei, Y., et al. (2009), Westward ionospheric electric field perturbations on the dayside associated with substorm processes, *J. Geophys. Res.*, *114*, A12209, doi:10.1029/2009JA014445.

Wei, Y., et al. (2010), Long-lasting goodshielding at the equatorial ionosphere, *J. Geophys. Res.*, *115*, A12256, doi:10.1029/2010JA015786.

Wei, Y., et al. (2011a), Responses of the ionospheric electric field to the sheath region of ICME: A case study, *J. Atmos. Sol. Terr. Phys.*, *73*, 123–129, doi:10.1016/j.jastp.2010.03.004.

Wei, Y., W. Wan, Z. Pu, M. Hong, Q. Zong, J. Guo, B. Zhao, and Z. Ren (2011b), The transition to overshielding after sharp and gradual interplanetary magnetic field northward turning, *J. Geophys. Res.*, *116*, A01211, doi:10.1029/2010JA015985.

Wilder, F. D., C. R. Clauer, and J. B. H. Baker (2009), Reverse convection potential saturation during northward IMF under various driving conditions, *J. Geophys. Res.*, *114*, A08209, doi:10.1029/2009JA014266.

Wolf, R. A., R. W. Spiro, S. Sazykin, and F. R. Toffoletto (2007), How the Earth's inner magnetosphere works: An evolving picture, *J. Atmos. Sol. Terr. Phys.*, *69*(3), 288–302, doi:10.1016/j.jastp.2006.07.026.

Yu, Y.-Q., and A. J. Ridley (2011), Understanding the response of the ionosphere-magnetosphere system to sudden solar wind density increases, *J. Geophys. Res.*, *116*, A04210, doi:10.1029/2010JA015871.

Yuan Z., and X. Deng, (2007), Effects of continuous solar wind pressure variations on the long-lasting penetration of interplanetary electric field during southward interplanetary magnetic field, *Adv. Space Res.*, *39*, 1342–1346, doi:10.1016/j.asr.2007.02.033.

Zhao, B., W. Wan, and L. Liu (2005), Response of equatorial anomaly to the October–November 2003 superstorm, *Ann. Geophys.*, *25*, 1555–1568.

Zhao, B., et al. (2008), Ionosphere disturbances observed throughout Southeast Asia of the superstorm of 20–22 November 2003, *J. Geophys. Res.*, *113*, A00A04, doi:10.1029/2008JA013054.

Zhao, B., et al. (2012), Positive ionospheric storm effects at Latin America longitude during the superstorm of 20–22 November 2003: Revisit, *Ann. Geophys.*, *30*, 831–840, doi:10.5194/angeo-30-831-2012.

Zong, Q.-G., B. W. Reinisch, P. Song, Y. Wei, and I. A. Galkin (2010), Dayside ionospheric response to the intense interplanetary shocks–solar wind discontinuities: Observations from the digisonde global ionospheric radio observatory, *J. Geophys. Res.*, *115*, A06304, doi:10.1029/2009JA014796.